Molecular Therapy
Original Article

Long-Term Persistence of Anti-HIV Broadly Neutralizing Antibody-Secreting Hematopoietic Cells in Humanized Mice

Anne-Sophie Kuhlmann,[1] Kevin G. Haworth,[1] Isaac M. Barber-Axthelm,[1] Christina Ironside,[1] Morgan A. Giese,[1] Christopher W. Peterson,[1,2] and Hans-Peter Kiem[1,2,3]

[1]Stem Cell and Gene Therapy Program, Fred Hutchinson Cancer Research Center, Seattle, WA, 98109-1024, USA; [2]Department of Medicine, University of Washington, Seattle, WA, 98195, USA; [3]Department of Pathology, University of Washington, Seattle, WA, 98195, USA

Broadly neutralizing antibodies (bNAbs) are among the most promising strategies to achieve long-term control of HIV-1 in the absence of combination antiretroviral therapy. Passive administration of such antibodies in patients efficiently decreases HIV-1 viremia, but is limited by the serum half-life of the protein. Here, we investigated whether antibody-secreting hematopoietic cells could overcome this problem. We genetically modified human CD34$^+$ hematopoietic stem and progenitor cells (HSPCs) to secrete bNAbs and transplanted them into immunodeficient mice. We found that the gene-modified cells engraft and stably secrete antibodies in the peripheral blood of the animals for the 9 months of the study. Antibodies were predominantly expressed by human HSPC-derived T- and B cells. Importantly, we found that secreted PGT128 was able to delay HIV-1 viremia *in vivo* and also prevent a decline in CD4$^+$ cells. Gene-modified cells were maintained in bone marrow and were also detected in spleen, thymus, lymph nodes, and gut-associated lymphoid tissue. These data indicate that the bNAb secretion from HSPC-derived cells in mice is functional and can affect viral infection and CD4$^+$ cell maintenance. This study paves the way for potential applications to other diseases requiring long-lasting protein or antibody delivery.

INTRODUCTION

Combination antiretroviral therapy (cART) has been a significant step toward a treatment of HIV but is not curative. Morbidities have been associated with these life-long treatments, and the ability of the cART drugs to reach latent viral reservoirs is unclear.[1,2] As a consequence, cART does not eradicate persisting HIV from latently infected cells in the reservoir compartments, and treatment interruption is invariably associated with viral rebound. To achieve cART-free virus remission, it will be necessary to more effectively target viral reservoirs, either by eradicating latently infected cells or preventing HIV replication following cART withdrawal. ART failure can be associated with mutations in critical broadly neutralizing antibodies (bNAbs) epitopes in the HIV envelope highlighting the importance of bNAbs and their relevance as a promising treatment option.[3] Several studies have reported an impact of bNAbs on viral reservoirs.[4–8] bNAbs can also efficiently target HIV-1 when administered as a pre- or post-exposure prophylactic.[9–16] While cART blocks *de novo* virus replication, bNAbs can neutralize circulating viral particles, actively target HIV-infected cells expressing the HIV envelope,[12,17] and stimulate the host immune response.[15,18]

The development of single B cell isolation and high-throughput antibody identification pipelines led to the characterization of a new generation of highly potent bNAbs and renewed interest in these therapies for HIV prophylaxis and cure. Several preclinical studies and clinical trials focused on intravenous administration of bNAb protein ("passive administration"), establishing the potential and safety profiles of these therapeutics as well as the absence of anti-antibody immune response.[13,19] However, despite efforts to engineer antibodies to improve their potency and half-life *in vivo*, bNAb persistence remains a substantial limitation both in nonhuman primate (NHP) models[20,21] and patients.[10,13,15,16,22] In simian/human immunodeficiency virus (SHIV)-infected rhesus macaques, multiple rounds of bNAb therapy during the acute phase of infection controlled viremia for up to 6 months before viral rebound was observed, correlating with decreasing plasma bNAb concentration.[18] Notably, the half-life of bNAbs in HIV-infected individuals is shorter than in healthy individuals, possibly due to a greater clearance of antigen-antibody immune complexes.[10,13,16] In summary, sustained antibody expression and delivery to viral reservoirs, although crucial for any impactful bNAb-based therapy, has yet to be achieved.

The use of gene-modified hematopoietic stem and progenitor cells (HSPCs) to express bNAbs has the potential to address these limitations. HSPCs differentiate into all lymphoid and myeloid lineages with the ability to cross physiological and anatomical barriers. As

Received 13 March 2018; accepted 20 September 2018;
https://doi.org/10.1016/j.ymthe.2018.09.017.

Correspondence: Hans-Peter Kiem, Stem Cell and Gene Therapy Program, Fred Hutchinson Cancer Research Center, Seattle, WA, 98109-1024, USA.
E-mail: hkiem@fredhutch.org

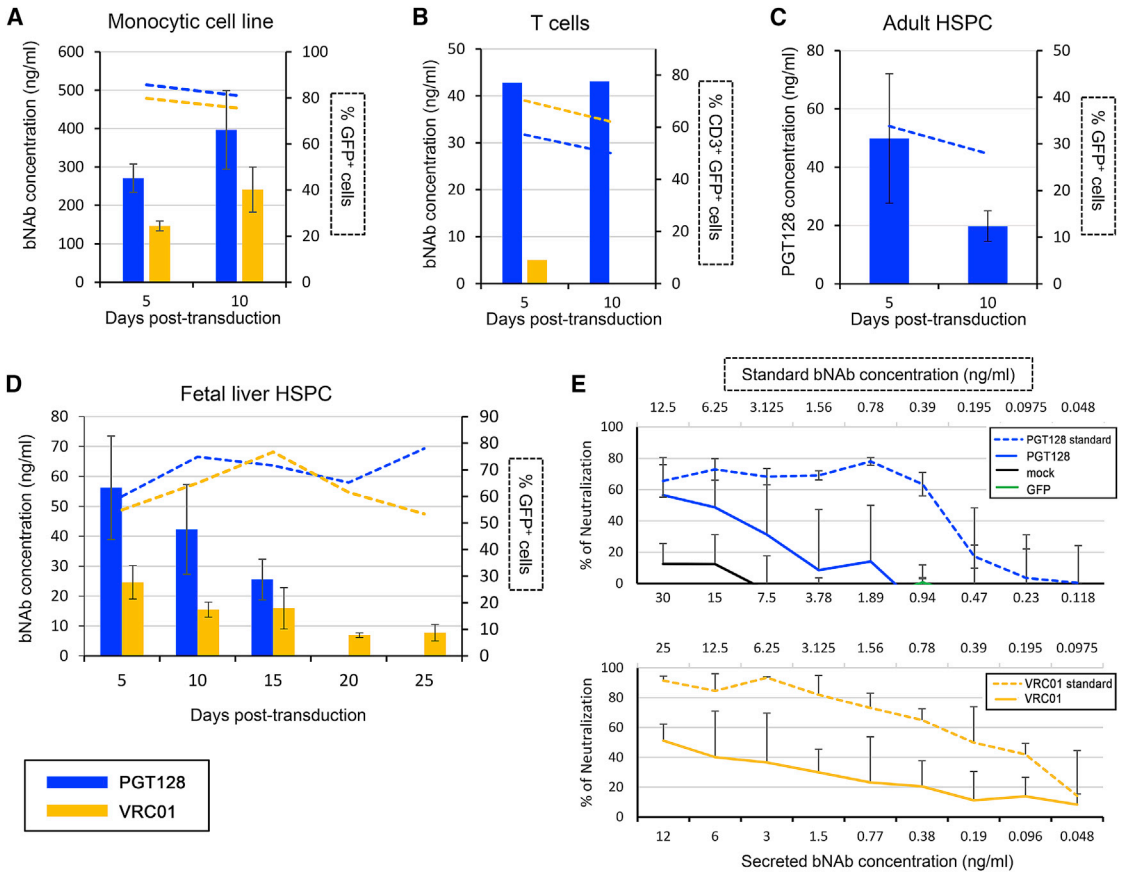

Figure 1. Human Hematopoietic Cells Can Secrete Broadly Neutralizing Antibodies *In Vitro*

PGT128 or VRC01 bNAb secretion by human THP-1 monocytic cell line (A), primary human CD3$^+$ T cells (B), adult (C), or fetal liver CD34$^+$ cells (D) was quantified by ELISA from cell-free supernatants at the indicated time points following transduction. GFP expression was determined at the same time points by flow cytometry and represented as dashed lines (right y axes). THP-1 cells were cultured at a cell density of 4×10^5 cells/mL, T cells at 2×10^6 cells/mL, and adult and fetal liver HSPCs at 1×10^6 cells/mL. (E) TZM-bl neutralization assay using cell-free supernatants harvested from the indicated human fetal liver cells (5 days post-transduction) measured at 2 days post-infection with HIV-1 BaL. Data are represented as means of two to three replicates from one representative experiment. Error bars represent SDs.

such, HSPC-based approaches represent a powerful tool to target latent viral reservoirs. Analogous strategies have already shown promise in the treatment of lysosomal storage disorders by delivering the functional arylsulfatase A (ARSA) enzyme to the central nervous system.[23] A phase I and II clinical trial has been initiated, and follow-up analyses indicate efficiency and safety of this life-long therapy. Most importantly, HSPCs' long-term persistence could support life-long remission without the need for ongoing cART. A previous study demonstrated the potential of hematopoietic cells to secrete anti-HIV bNAbs and protect against HIV infection.[24] However, *in vivo* properties of these cells, including long-term engraftment, persistent bNAb secretion, and delivery of bNAbs to the reservoir tissues, have not been explored yet. Here, we employed bNAb-expressing lentiviral vectors to investigate the long-term secretion and functional trafficking of bNAb-modified hematopoietic cells in humanized mice. Our results provide a key step forward in the advancement of cell-based bNAb delivery strategies to HIV$^+$ patients.

RESULTS

Hematopoietic Cells Secrete Functional bNAbs *In Vitro*

We first investigated the potential of cultured cell lines and primary cells, including human CD34$^+$ cells, to secrete functional bNAbs. To characterize the ability of lymphoid and myeloid cells to secrete bNAbs, the monocytic cell line THP-1 and isolated primary human CD3$^+$ T cells were transduced with lentiviral vectors encoding either PGT128 or VRC01 bNAbs in combination with GFP (Figure S1). The monocytic THP-1 cell line was efficiently transduced after 5 and 10 days, with 86% and 81% of cells being GFP$^+$ in the PGT128 condition and 80% and 75% GFP$^+$ cells in the VRC01 condition (Figure 1A). THP-1 cells produced 271 and 397 ng/mL of PGT128 at 5 and 10 days post-transduction, respectively, and 146 and 241 ng/mL of VRC01 were detected at the same time points (Figure 1A). Isolated T cells were also efficiently transduced (Figure 1B). Five and ten days following the transduction, 57% and 50% of the PGT128-transduced T cells and 70% and 62% of the VRC01-transduced CD3$^+$ cells expressed GFP (Figure 1B). Approximately 40 ng/mL of PGT128 was

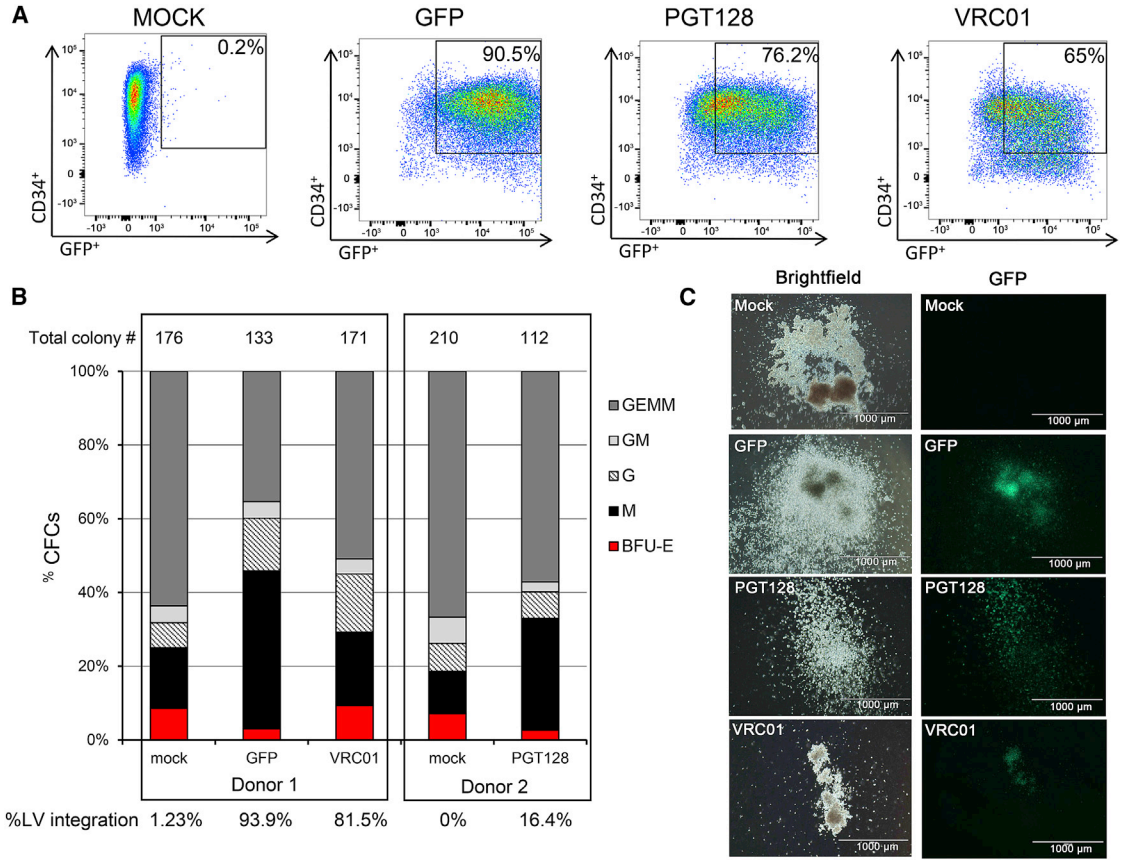

Figure 2. Characterization of bNAb-Modified HSPCs

(A) GFP expression in human fetal liver CD34$^+$ cells, analyzed 1 day post-transduction. (B) CD34$^+$ colony assays. The percentages of erythroid (BFU-E), granulocyte-macrophage (GM, G, and M), and multipotent granulocyte, erythroid, macrophage, and megakaryocyte (GEMM) progenitor colonies are indicated. Total number of colonies per condition is indicated above the histograms, and percentage of lentivirus (LV)-positive colonies, quantified by PCR, is indicated below. (C) Representative images of colony morphology and GFP expression for each group. Scale bar, 1 mm.

quantified at 5 and 10 days post-transduction, while VRC01 was detected at 5 days post-transduction but not detected at 10 days (Figure 1B). Adult or fetal liver (FL) human CD34$^+$ cells were next transduced with our vectors. Five to ten days after transduction with PGT128 vectors, 34% and 28% of the adult CD34$^+$ cells expressed GFP and produced 50 ng/mL to 20 ng/mL of PGT128 bNAb in the supernatant, respectively (Figure 1C). Similarly, 60% to 78% of the human FL CD34$^+$ cells transduced with the PGT128 construct were GFP$^+$ between 5 and 25 days post-transduction (Figure 1D). VRC01 vector transduction efficiencies ranged from 53% to 77% (Figure 1D). bNAb secretion in the supernatant was measured by ELISA and detected as early as 5 days post-transduction for both PGT128 (56 ng/mL) and VRC01 (25 ng/mL) (Figure 1D). bNAbs were detected for up to 25 days post-transduction in the case of VRC01 and until 15 days post-transduction in the case of PGT128. The function of the secreted bNAbs collected from FL CD34$^+$ cells supernatants at 5 days post-transduction were then assessed in a neutralization assay and compared with standard purified monoclonal bNAbs. HIV-1 BaL averaged 50% neutralization in the presence of 12–15 ng/mL of VRC01 and PGT128 secreted bNAbs, respectively (Figure 1E). Collectively, these data demonstrate the potential of differentiated lymphoid and myeloid cells as well as human HSPCs to secrete functional bNAbs *in vitro* following lentivirus-mediated gene modification.

bNAb-Secreting Cells Engraft and Persist Long Term in Humanized Mice

We next assessed the ability of antibody-secreting HSPCs and their progeny to engraft and persist in a humanized mouse model. NSG neonate mice were infused with gene-modified human CD34$^+$ cells 1 day post-transduction (Figure S2). The phenotype and differentiation potential of the infused cells were characterized in parallel *ex vivo* (Figures 2 and S3). One day post-transduction, 90.5% of the cells transduced with GFP-only lentiviral particles were CD34$^+$GFP$^+$ (Figure 2A). Cells transduced with PGT128-GFP or VRC01-GFP lentiviruses were 76.2% and 65% CD34$^+$GFP$^+$, respectively (Figure 2A). Additionally, the CD34$^+$CD45RA$^-$CD90$^+$ population of HSPCs recently identified as long-term persisting and containing

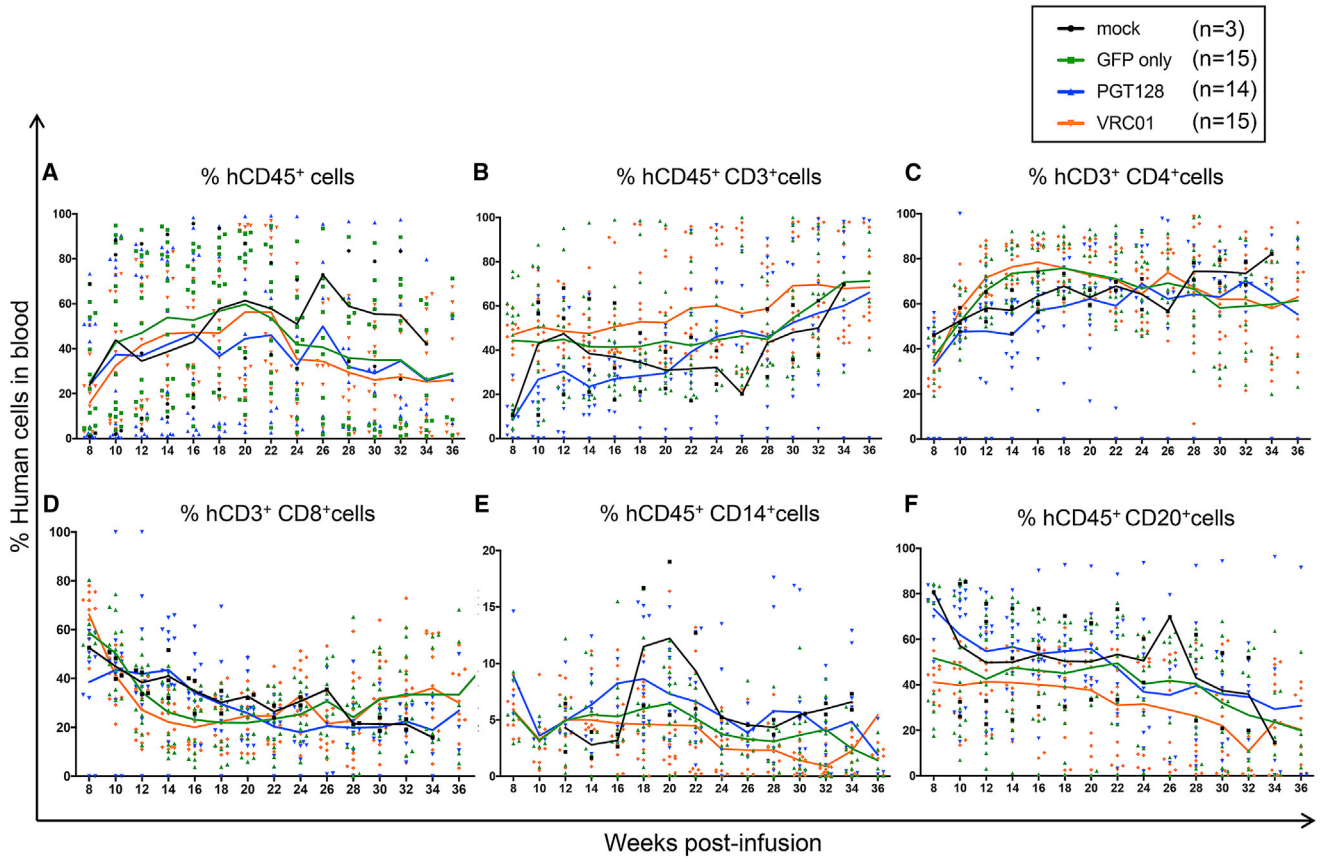

Figure 3. Total Human CD34$^+$ HSPCs Engraft in NSG Mice

Engraftment in peripheral blood was analyzed at the indicated time points by flow cytometry in the following lineages: (A) total human CD45$^+$, (B) human CD45$^+$CD3$^+$, (C) human CD45$^+$CD3$^+$CD4$^+$, (D) human CD45$^+$CD3$^+$CD8$^+$, (E) human CD45$^+$CD14$^+$, and (F) human CD45$^+$CD20$^+$. Each symbol represents an individual mouse with solid lines representing the mean for each group. Individual engraftment data can be found in Figure S6.

multi-lineage potential[25] was as efficiently transduced as the other progenitors (Figure S4). In colony-forming cell (CFC) assays, both antibody-producing and mock cells gave rise to similar proportions of various progenitor populations (Figures 2B and 2C). Quantification of lentiviral gene marking showed higher percentages in GFP-only modified colonies compared to the bNAb-GFP constructs, likely because the smaller GFP-only vector integrated more efficiently than the dual bNAb-GFP vectors (Figure 2B). Analysis of engraftment and persistence of both the total human cell population and GFP$^+$ gene-modified cells in the peripheral blood of NSG mice were initiated 2 months post-infusion (Figures 3, 4, S5, and S6). Similar to previously published data from our group,[26] the human CD45$^+$ cell populations were stable over time (Figure 3A). The percentage of total human CD45$^+$, CD3$^+$, CD4$^+$, CD8$^+$, CD20$^+$, and CD14$^+$ cells were not significantly different between the mock, GFP-only, and antibody-producing cohorts (Figures 3A–3F). Importantly, all analyzed lineages persisted through necropsy at approximately 36 weeks post-infusion. The percentage of GFP$^+$ gene-modified cells were also detected in all analyzed lineages until the end of the experiment, and longitudinal analyses demonstrated the stability of the engraftment in all groups (Figure 4). The GFP-only group exhibited an average of 74% engraftment of CD45$^+$GFP$^+$ at 8 weeks to 58% at 36 weeks, while the PGT128 group showed 40% CD45$^+$GFP$^+$ at 8 weeks and 24% at 36 weeks, and the VRC01 group was 12% CD45^{+-}GFP$^+$ at 8 weeks and 15% at 36 weeks (Figure 4A). Greater proportions of the gene-modified cells in the GFP-only group relative to the bNAb-producing groups was observed in all lineages, consistent with our *ex vivo* data (Figure 2). However, gene-modified cells from all groups engrafted and persisted for up to 9 months in the peripheral blood in all the analyzed lineages (CD45$^+$, CD3$^+$, CD4$^+$, CD8$^+$, CD14$^+$, and CD20$^+$ cells). These data demonstrate that gene-modified, bNAb-secreting cells engraft and persist *in vivo* in the peripheral blood of humanized mice for the duration of each animal's study.

Gene-Modified Cells Are Found in Lymphoid Tissues

A critical advantage of our HSPC-based bNAb delivery method is the ability to deliver the therapeutic product to secondary tissue sites of HIV persistence via differentiated myeloid and lymphoid progeny. Therefore, we next quantified the levels of gene-modified cells in these tissues at necropsy. At study end point, gene-modified GFP$^+$ cells

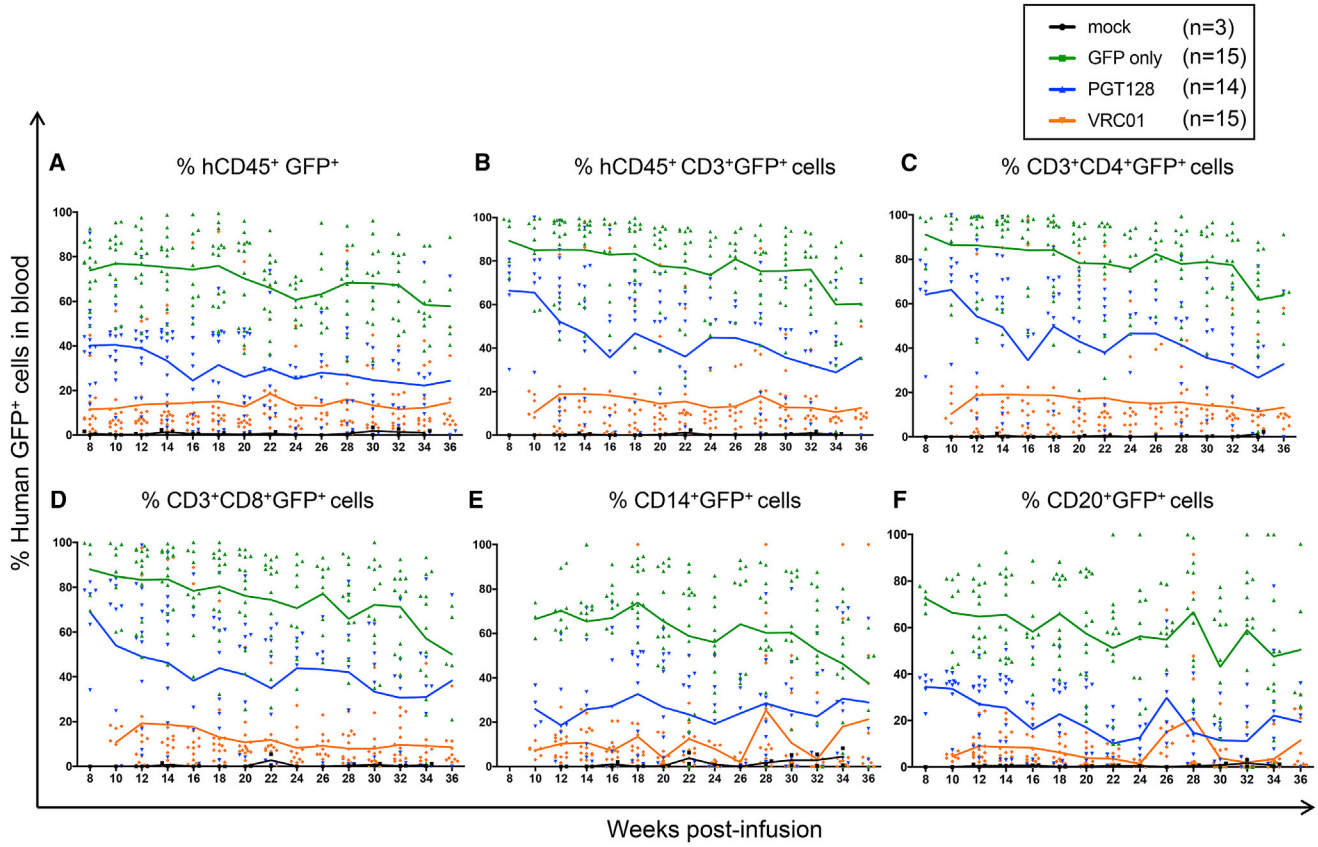

Figure 4. Gene-Modified Human CD34$^+$ HSPCs Engraft in NSG Mice

The engraftment of the GFP$^+$ gene-modified cells in the peripheral blood was analyzed at the indicated time points by flow cytometry in the following lineages: (A) human CD45$^+$GFP$^+$, (B) human CD45$^+$CD3$^+$GFP$^+$, (C) human CD3$^+$CD4$^+$GFP$^+$, (D) human CD3$^+$CD8$^+$GFP$^+$, (E) human CD45$^+$CD14$^+$GFP$^+$, and (F) human CD45$^+$CD20$^+$GFP$^+$. Each symbol represents an individual mouse, with solid lines representing the mean for each group. Individual engraftment data can be found in Figure S6.

were detected not only in the peripheral blood, (Figure 5A) but also in the spleen, thymus, and bone marrow of GFP-only, PGT128, and VRC01 mice (Figures 5B–5D) and were found in multiple human CD45$^+$ subsets, including CD34$^+$, CD3$^+$, CD4$^+$, CD8$^+$, CD20$^+$, and CD14$^+$ cells (Figures 5A–5D). As observed during the longitudinal peripheral blood analyses, the GFP-only cells were detected at a higher percentage; bNAb-producing cells also achieved persistent engraftment, albeit at a lower level. Bone marrow cells isolated at necropsy from GFP-only and bNAb-producing mice reconstituted burst-forming unit (BFU)-E, -M, -G, -GM, and -GEMM progenitors, and PCR analyses confirmed that the cells were still gene modified (Figure 5E). We next used immunohistochemistry-based methods to confirm that these cells were tissue resident. GFP staining was specific to animals receiving gene-modified HSPCs (Figure 6). GFP$^+$ cells were detected in the spleen (Figure 6A), the lamina propria, and intestinal submucosa of the small intestine (Figure 6B), the mesenteric lymph nodes (Figure 6C), and in gut-associated lymphoid tissues (GALT) from small intestine (Figure 6D). These data demonstrate that the gene-modified cells maintain trafficking and engraftment in HIV reservoir tissues despite modification for bNAbs production.

Sustained Antibody Secretion Is Detected in the Peripheral Blood

Following demonstration of the efficient engraftment, persistence, and trafficking of gene-modified cells in humanized mice, we next evaluated the ability of these cells to secrete bNAbs *in vivo*. Starting at 2 months post-infusion, plasma bNAbs were quantified by ELISA in the mice expressing VRC01 or PGT128 relative to GFP-only mice. Secreted PGT128 and VRC01 bNAbs could be detected as early as 8 weeks (Figures 7A and 7B). Between 14 and 20 weeks, both PGT128 and VRC01 concentrations increased up to 388 ng/mL of PGT128 and 90 ng/mL of VRC01 (Figures 7A and 7B). Starting at 20 weeks post-infusion, bNAb concentrations stabilized with an average of 63 ng/mL of PGT128 and 20.6 ng/mL of VRC01 for up to 9 months post-infusion (Figures 7A and 7B). Several PGT128 mice that initially presented detectable secretion of bNAbs became negative at later time-points. To determine whether this was due to a loss of bNAb production, bNAb mRNA expression was analyzed in total white blood cells. Both heavy- and light-chain variable regions of PGT128 were detected in animals that were negative by ELISA at 32 weeks (Figure 7C). Similar results were seen in ELISA-negative

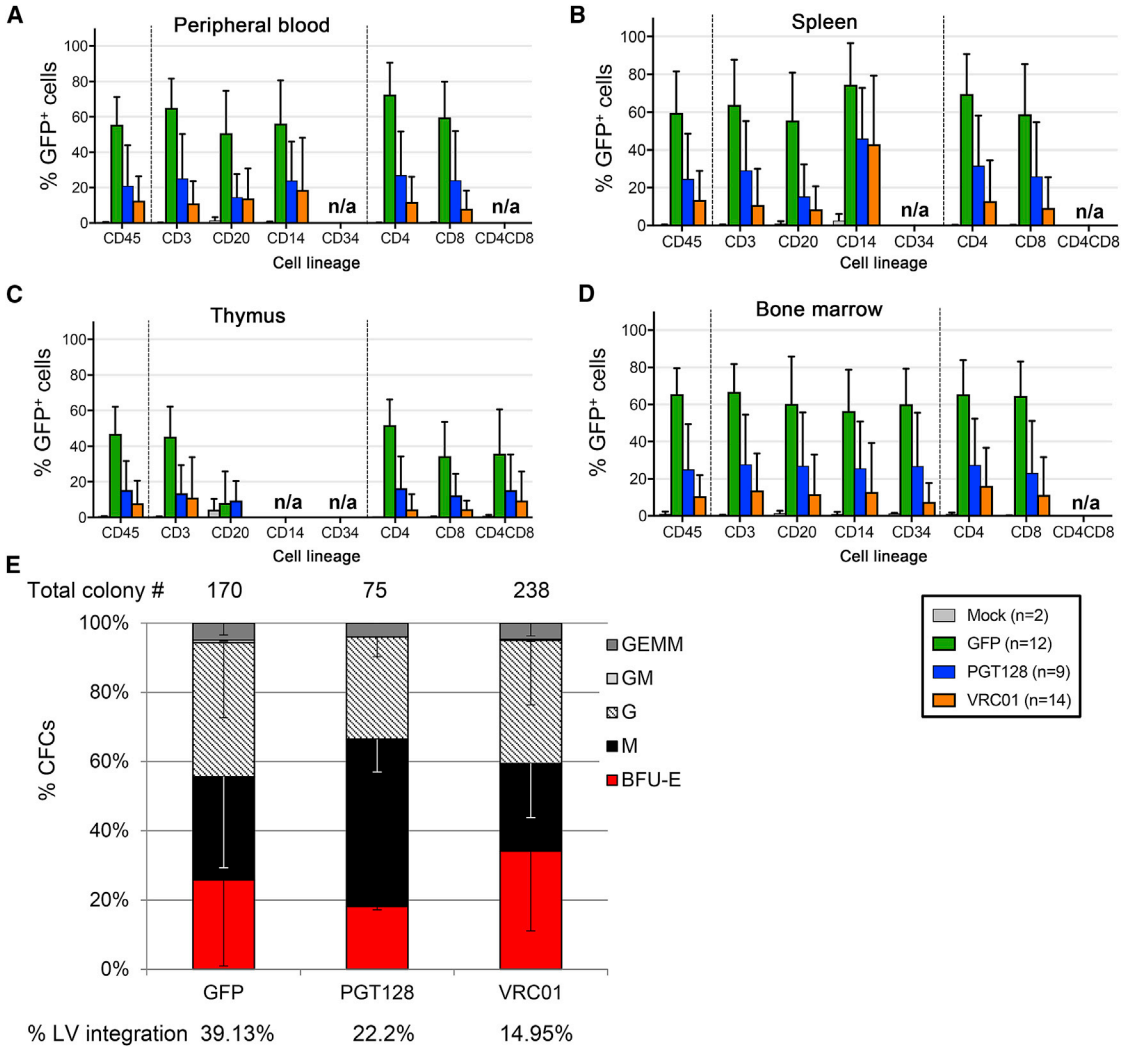

Figure 5. Human CD45 Subset Distribution in Engrafted NSG Mice at Study End Point

(A–D) The percentage of GFP$^+$ cells of the indicated lineages were analyzed by flow cytometry in the peripheral blood (A), spleen (B), thymus (C), and bone marrow (D) at necropsy (34 and 36 weeks post-infusion). Data are represented as means of four cohorts of mice. Error bars represent SDs. n/a, not applicable, means undetectable cells in the indicated lineages. (E) Total bone marrow cells were analyzed via colony assay and the percentages of erythroid (BFU-E), granulocyte-macrophage (GM, G and M), and multipotent granulocyte, erythroid, macrophage, and megakaryocyte (GEMM) progenitor colonies are indicated. Total number of colonies per condition is indicated above the histograms, and percentage of lentivirus (LV)-positive colonies, quantified by PCR, is indicated below. Data are represented as means of three replicates within one representative experiment. Error bars represent SDs.

VRC01 mice analyzed at the time of necropsy (Figure 7D). Additionally, plasma bNAb decline was associated with a decrease in the number of bNAb-modified cells (human CD45$^+$ and CD45$^+$GFP$^+$ cells) (data not shown). Overall, these data demonstrate sustained antibody secretion.

Characterization of bNAb Production by the Lymphoid or Myeloid Lineages

Characterizing which HSPC-derived lymphoid and myeloid lineages best support bNAb secretion *in vivo* is critical in order to understand the potential of the different cell types to systemically deliver these therapeutics. Cells were not available in sufficient quantities for subsequent cell culture and analysis of antibody secretion in the supernatant. Therefore, we analyzed bNAb mRNA expression from sorted subsets. bNAb heavy- and light-chain variable regions were detected in the human T and B cells from VRC01 (Figure S7A) and PGT128 (Figure S7B) cohorts, in contrast to the GFP-only groups. bNAb mRNA could not be amplified in myeloid lineage cells, likely due to the low number of CD14$^+$ myeloid cells available as a result of the lower reconstitution of the myeloid lineage in our model (Figure 3E). Nevertheless, our data show that, at minimum, HSPC-derived CD3$^+$ and CD20$^+$ lymphocytes have the potential to produce bNAbs.

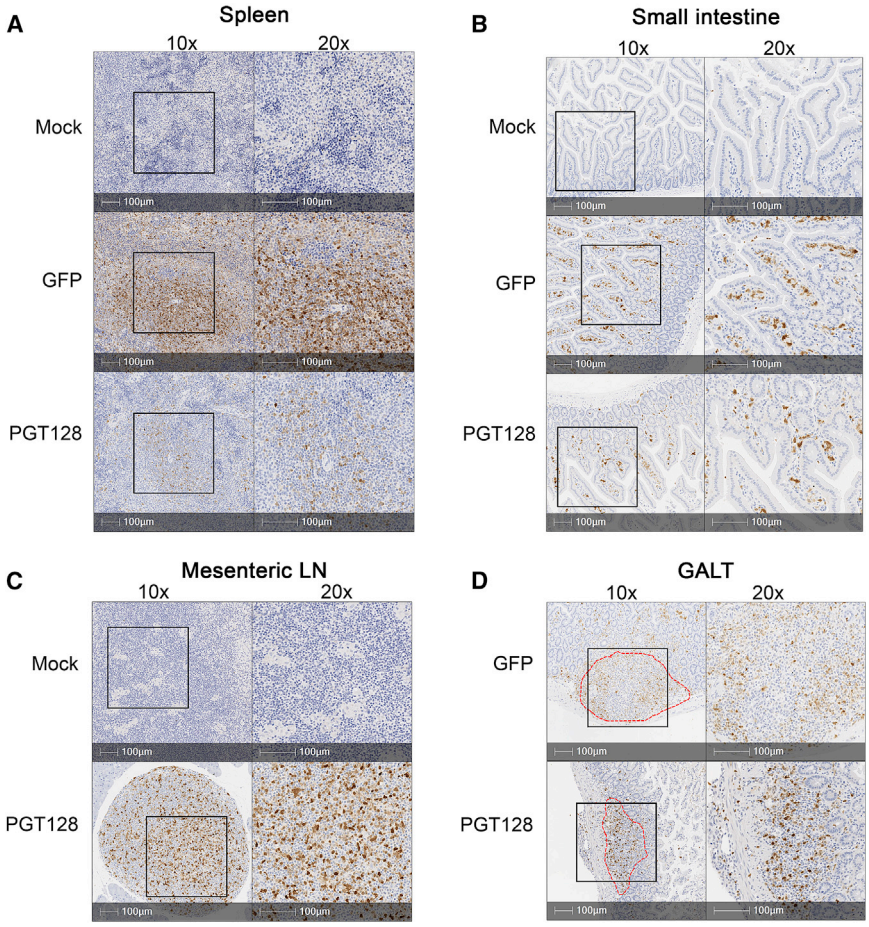

Figure 6. Gene-Modified Human CD34⁺-Derived Cells Traffic to Tissues

Anti-GFP IHC staining of the GFP⁺ gene-modified cells in the spleen (A), small intestine (B), mesenteric lymph nodes (LN) (C), and GALT (D) from mock, GFP-only, or PGT128-GFP mice. Red dotted lines, GALT. Right, 20× magnification from the indicated region of the left (10× magnification). Tissues were collected at necropsy, 34 weeks post-infusion.

Secreted bNAbs Are Functional *In Vivo*

Finally, to determine if the detected concentrations of VRC01 and PGT128 bNAbs would be sufficient to impact HIV viremia, mice from the GFP-only and bNAb-producing groups were challenged with HIV-1 between 19 and 23 weeks post-infusion. Viremia could be detected as early as 2 weeks following the challenge (Figure 8A). Even though not significant, the onset of viremia was delayed in the PGT128 mice compared to the GFP and VRC01 groups (Figure 8A). In contrast, viremia in the VRC01 group was earlier than in the GFP-only and PGT128 mice, which is likely explained by the respective IC_{50} of PGT128 and VRC01 for our challenge virus HIV-1 BaL, which differs substantially for the two antibodies and with better inhibition for PGT128 (see Discussion). Follow-up of the mice showed that more animals from the PGT128 group remained aviremic until 10 weeks following the infection than in the VRC01 and GFP-only groups (Figure 8B). Figure 8C shows the impact of HIV infection on $CD4^+$ cell frequencies in mice. Both the GFP-only and VRC01 groups showed a significant decrease in $CD4^+$ cells, while such a decline was not seen in the PGT128 group. Overall, these data indicated that the HSPC-derived secretion of bNAbs is functional *in vivo* and can affect viral infection and $CD4^+$ cell maintenance.

DISCUSSION

Our strategy addresses two challenges of HIV treatment: (1) sustained levels of a curative therapeutic and (2) local delivery to relevant secondary sites beyond peripheral blood. We show that human HSPCs genetically modified to secrete bNAbs engraft and persist in peripheral blood and tissues of humanized mice, modified cells are tissue-resident, and HSPC-derived T and B cells contribute to bNAb production.

Both human FL and adult $CD34^+$ cells secreted bNAbs following *ex vivo* lentivirus-mediated gene insertion in our study. When infused *in vivo*, the engraftment efficiencies and lineage distributions were similar between secreting and non-secreting mice. More gene-modified GFP^+ cells were detected in the GFP-only mice relative to the bNAb-groups in all tested lineages. This difference in GFP detection was observed as early as 1 day post-transduction and can be explained by the shorter size of the GFP-only construct relative to the bNAb-encoding construct allowing greater transduction efficiency. This is in agreement with the higher lentiviral integration detected pre- and post-infusion. Following successful engraftment, secreted bNAbs could be detected in the plasma as early as 8 weeks and reached a plateau after 20 weeks of infusion. Higher engraftment of both $CD45^+$ and $CD45^+GFP^+$ cells led to higher antibody secretion, while no antibody could be detected by ELISA in mice with lower engraftment despite detectable mRNA expression using a more sensitive PCR assay. Importantly, bNAb-secreting cells maintained engraftment and multi-lineage potential, as well as ability to persist *in vivo*.

The promise of protein secretion and local delivery was demonstrated in gene therapy for lysosomal storage disorders in a phase I and II clinical trial, establishing the long-term safety and efficiency in patients.[23] In a preclinical mouse model, functional enzyme delivery and activity was observed in different tissues such as spleen, liver, or central nervous system[27,28] leading to improvement of symptoms.[29] Our study also demonstrates the presence of gene-modified GFP^+ cells in the spleen, thymus, bone marrow, lymph nodes, and

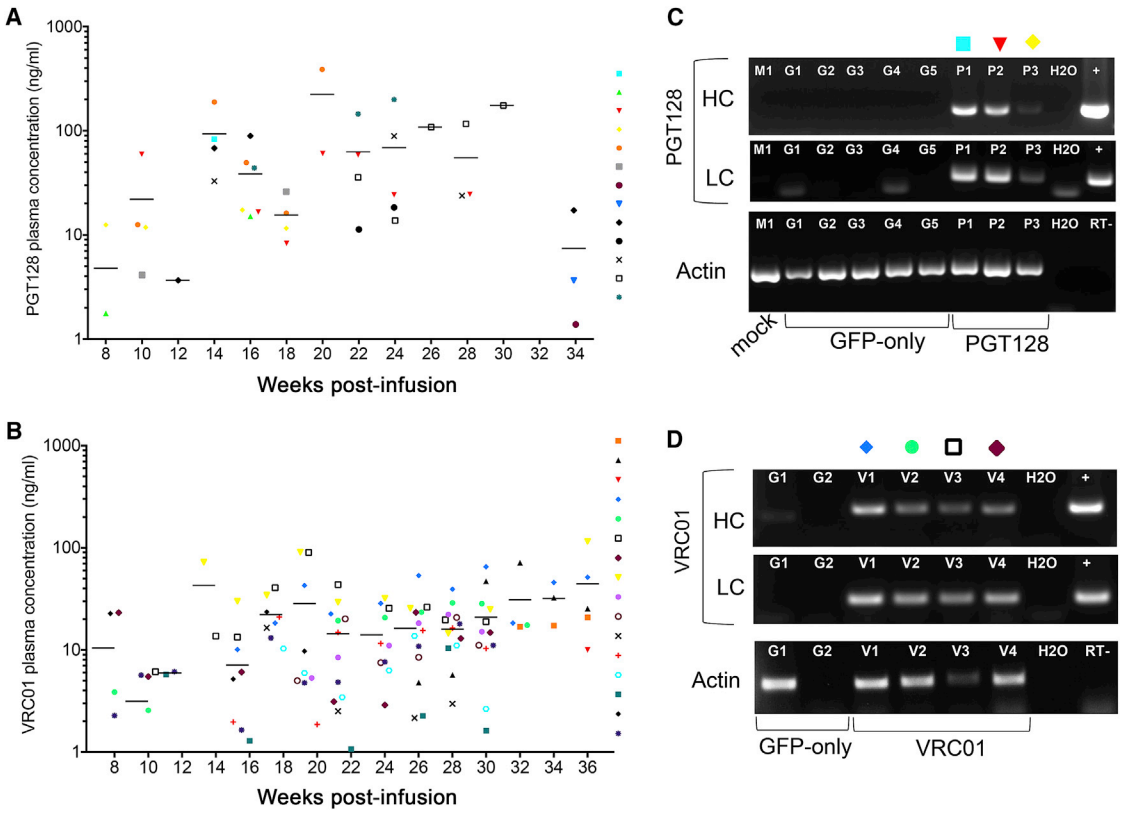

Figure 7. Persistent bNAb Secretion *In Vivo*

Plasma concentrations of secreted PGT128 (A) or VRC01 (B) antibodies detected by ELISA from four different cohorts of humanized mice at the indicated time points. Each symbol represents an individual mouse with solid lines representing the mean for each time point. (C) mRNA expression of PGT128 antibody heavy chain (HC, top), light chain (LC, middle), and actin (bottom) were measured by RT-PCR at 32 weeks in the mock (n = 1, M1), GFP-only (n = 5, G1 to G5), and PGT128 (n = 3, P1 to P3) mice. (D) Same as (C) for VRC01-modified mice, 33 weeks (V2) and 36 weeks: GFP-only (n = 2, G1 and G2), and VRC01 (n = 4, V1 to V4). H2O, water negative control; RT−, no reverse transcriptase; +, bNAb-encoding plasmid positive control.

gastrointestinal tract including GALT several months following the infusion of bNAb-modified HSPCs, indicating maintenance of trafficking ability despite cell modification for bNAb production. Our data strongly support the premise that HSPC-based delivery of bNAbs could facilitate effective local antibody delivery to relevant HIV reservoir tissues.

The bNAb concentrations detected in peripheral blood in our study ranged from 20 to 60 ng/mL to a maximum of 400 ng/mL. In the context of HIV-1 and based on previous studies in mice,[8,30] and NHP,[18,30,31] we estimate that a threshold concentration of 5 to 10 μg/mL might be required to prevent or delay the viral rebound, while a minimum of 50 to 100 μg/mL seems necessary to durably impact plasma viremia in HIV-infected patients,[13,32] suggesting that higher concentrations of secreted bNAbs may have to be achieved to reach a therapeutic level. These concentrations will likely vary in each individual depending on the viral strain, time post-infection, size of the reservoir, the type of bNAb being used (breadth and potency of neutralization, Fc-mediated effector functions, pharmacokinetic properties, etc.), and levels of the antibody in reservoir tissues.

Importantly, more efficient delivery of secreted bNAbs to reservoir sites via our HSPC-based approach may facilitate lower effective plasma concentrations relative to those required for efficacy in passive intravenous administration trials. In support of this hypothesis is the finding that the secreted PGT128 delayed the onset of HIV-1 viremia in contrast to the GFP-only mice, despite concentrations in the peripheral blood below 1 μg/mL. Further support is provided in Figure S8 which shows that passive antibody administration of PGT128 bNAb was able to delay onset of HIV replication despite concentrations below 1 μg/mL (Figure S8). Secreted VRC01 was associated with an increased viremia as early as 2 weeks following the challenge, possibly explained by suboptimal concentrations of VRC01 similar to previous observations with antibodies directed against the CD4-binding site epitope.[33] Other explanations might be the use of a different viral isolate in our study or different inhibitory concentrations, as PGT128 median IC_{50} is 10-fold lower than VRC01 IC_{50} when tested on a panel of pseudoviruses representing major circulating HIV subtypes.[34] Additionally, PGT128 concentrations lower than 100 ng/mL neutralized 50% of the tested viruses against 20% for VRC01.[34] Effective concentrations might even be lower

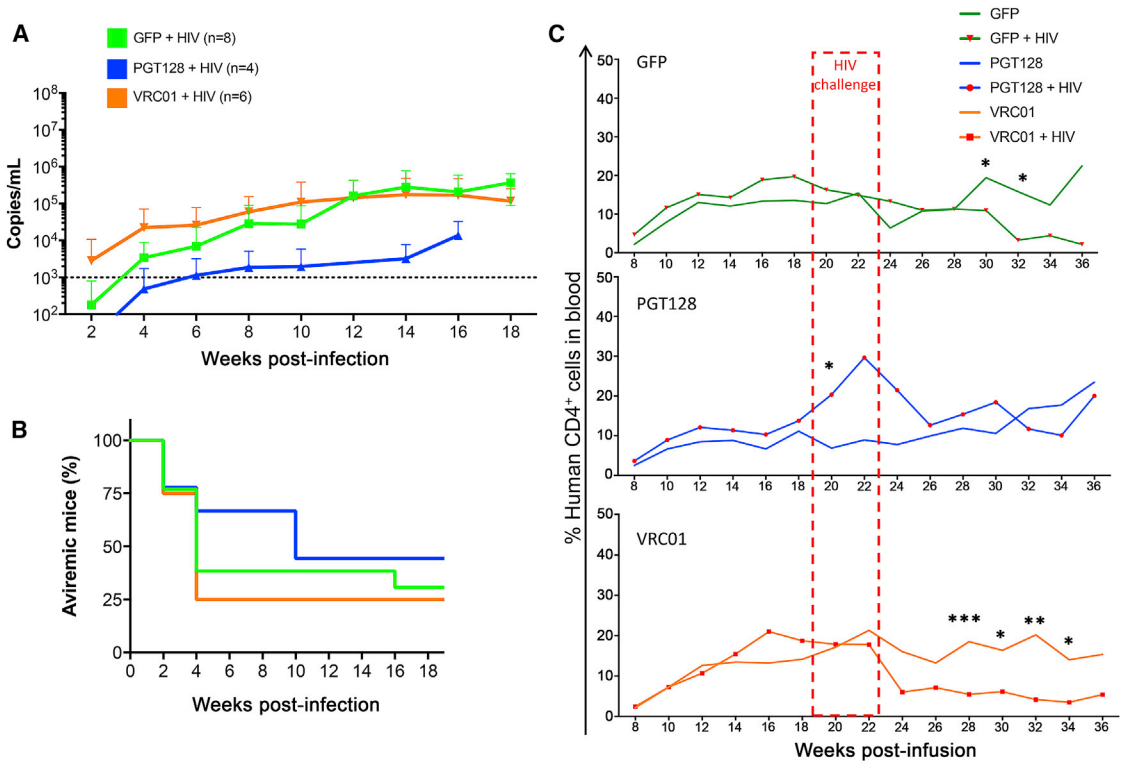

Figure 8. PGT128- and VRC01-Secreted Antibodies Impact HIV-1 Bal Viremia

(A) Plasma viral RNA was isolated from infected mice at the indicated time points and quantified by PCR to determine the average viremia (copies/mL) in challenged mice. Viremia was normalized to the percentage of total human $CD4^+$ cells in the peripheral blood at the same time points. Dashed line indicates threshold from background noise. Error bars represent SDs. (B) Aviremic mice that were challenged in the same experiments are represented. (C) Percentages of total human $CD4^+$ cells detected in the peripheral blood in uninfected or infected mice were determined by flow cytometry at the indicated time points before and following HIV challenge between 19 and 23 weeks post-infusion. Unpaired t test statistics were performed using GraphPad Prism. *$p < 0.05$; **$p < 0.01$; ***$p < 0.001$.

when conjugated with a stimulated host immune response.[15,18] For instance, a combination of secreted bNAbs selected based on their ability to bind to different epitopes, to neutralize the strain of interest, and their capacity to trigger Fc-mediated effector functions in the different tissues could further maintain cART-independent virus remission.[35,36] Bi-[37] and tri-specific[38] engineered bNAbs are also promising alternatives.

Characterizing the contribution of each hematopoietic lineage to bNAb secretion will be essential in maximizing the therapeutic threshold of our approach. Due to the limited amount of peripheral blood samples obtained from our humanized mouse model, we were not able to establish the secretion potential of the circulating isolated T cells, B cells, and monocytes *ex vivo*. However, bNAb mRNA production was detected in T and B cells in our study. Additional studies in larger animal models such as non-human primates will be necessary to address these limitations. Different approaches were assessed using non-lineage-specific[24,39] or B-cell-specific promoters[40–42] and demonstrated the ability of *ex vivo*-modified hematopoietic cells to secrete bNAbs *in vitro* and *in vivo*. Exogenous human factor IX was also secreted from gene-modified erythroid cells.[43] In accordance with our *in vitro* data, the capacity of human $CD3^+$ T cells to secrete antibodies *in vitro* was observed at similar concentrations (i.e., 30–40 ng/mL).[44] Collectively, these findings suggest that therapeutic levels of secreted bNAbs may be achieved by adapting bNAb promoters to the cells in which they are efficiently produced, with the goal of finding an optimum range of expression that balances efficacy, persistence, and local delivery.

Because the existence of viral reservoirs has not been established in our humanized mouse model, especially in the absence of ART, the impact of bNAb secretion on the reservoir size was not evaluated in this study. However, analysis of the trafficking of gene-modified bNAb-secreting cells to relevant tissues in an ART-treated animal model[45] will be critical to target the HIV reservoir sites. Secreting $CD4^+$ T cells would be an optimal delivery lineage, as they would co-localize with HIV^+ T cells, for example, in lymph node (LN) follicles[46] and could also act in combination with cytolytic $CD8^+$ T cells at these sites.[47] Although the ability of $CD8^+$ T lymphocytes to secrete bNAbs remains to be demonstrated, their trafficking to the LN following *ex vivo* gene modification in HIV-infected individuals has been established.[48] $CD8^+$ T lymphocytes can persist as tissue-resident long-lived

memory T cells in the gastrointestinal mucosa.[49] As such, it is conceivable that gene-modified memory CD8$^+$ T cells could constitute a persistent source of therapeutic bNAb-secreting cells, whose reactivation and proliferation could be antigen inducible. T cell-mediated bNAb secretion could be challenged by an increased risk of HIV infection, especially in light of our observations with suboptimal VRC01 concentrations and similar to previous data with anti-HIV CAR T cells, for instance.[50] T cell protection by C-C chemokine receptor 5 (CCR5)-locus disruption or expression of anti-HIV genes has the potential to address these issues, as described recently.[50]

Our strategy could facilitate targeting of re-activated infected cells from the latent viral reservoirs in secondary tissue compartments following cART withdrawal and could be combined with latency reversing agents.[8] An ideal treatment would initiate a combination of cART and passive bNAb administration early enough following infection to limit the seeding of HIV reservoirs, as suggested recently.[18,51] Transplantation of bNAb-encoding HSPCs would occur prior to cART treatment withdrawal, thus preventing or potently neutralizing viral replication following treatment interruption. Our study establishes the promising potential of bNAb-secreting cells using HSPC-based therapy to develop a cART-free HIV functional cure. Furthermore, gene therapy for cell-mediated delivery of therapeutics has a broad potential for applications and could be applied to several diseases requiring life-long prophylactic or therapeutic measures.

MATERIALS AND METHODS

Cells

Human FL CD34$^+$ HSPCs were obtained from Advance Bioscience Resources (ABR, Alameda, California). FL tissue was dissociated, and CD34$^+$ cells were enriched by immunomagnetic separation (IMS) according to the manufacturer's protocol (Miltenyi Biotec, Bergisch Gladbach, Germany). Isolated CD34$^+$ cells were cryopreserved for later use. Following thawing, CD34$^+$ cells were cultured in StemSpan serum-free expansion media (SFEM) (StemCell Technologies, Vancouver, BC, Canada), supplemented with stem cell factor (SCF), thrombopoietin (TPO) and Fms-related tyrosine kinase 3 ligand (FLT3-L; 100 ng/mL each), and 1% penicillin and streptomycin (Life Technologies, Grand Island, NY). Human apheresis CD34$^+$ HSPCs were isolated from total apheresis products purchased from the Cell Processing Facility at the Fred Hutchinson Cancer Research Center using the CliniMACS Prodigy device (Miltenyi Biotec), using previously described protocols.[52] CD34$^+$-enriched populations were characterized by flow cytometry using CD34 (clone 563), CD45RA (clone 5H9), and CD133 (clone AC133) antibodies. Negative fractions from isolated CD34$^+$ products were used for sequential autologous CD3$^+$ isolation using a positive selection kit according to manufacturer's protocol (Miltenyi Biotec) and were cryopreserved for later use. TZM-bl cells were obtained from the NIH AIDS reagent program (Dr. John C. Kappes, Dr. Xiaoyun Wu, and Tranzyme) and cultured in DMEM supplemented with 10% fetal bovine serum, 1% penicillin and streptomycin. THP-1 ATCC cells (NIH AIDS Reagent program, Drs. Li Wu and Vineet N. KewalRamani) were maintained in RPMI 1640 supplemented with fetal bovine serum 10%, 1 mM sodium pyruvate, and 0.05 mM 2-mercaptoethanol.

Lentivirus Production and Transduction

Self-inactivating (SIN) lentiviruses were produced using a third-generation packaging system and pseudotyped with the vesicular stomatitis virus G envelope (VSV-G). Vectors were produced by our institutional Vector Production Core (director, Hans-Peter Kiem) at the Fred Hutchinson Cancer Research Center. Infectious titer was determined by flow cytometry, quantifying eGFP expression in HT1080 human fibrosarcoma-derived cells transduced in the presence of 8 μg/mL of protamine sulfate. Human CD34$^+$ cells were thawed and incubated overnight at 37°C prior to transduction with titered vectors. Cells were plated in non-tissue culture (TC) treated, retronectin-coated plates. After a 45-min incubation, lentivirus was added at an MOI of 10 and incubated for 24 hr at 37°C.

CFC Assay

One day post-transduction, CD34$^+$ cells were seeded in triplicate in MethoCult H4435 (StemCell Technologies, Vancouver, Canada) containing recombinant human cytokines including SCF, interleukin-3 (IL-3), IL-6, erythropoietin (EPO), granulocyte colony-stimulating factor (G-CSF), and granulocyte-macrophage colony-stimulating factor (GM-CSF). At necropsy, cells isolated from bone marrow (BM) were seeded in triplicate into ColonyGEL (ReachBio, Seattle WA). Hematopoietic colonies were scored after 10–14 days. Counted colonies were identified as erythroid (BFU-E), granulocyte-macrophage (GM, G and M), or multipotential granulocyte, erythroid, macrophage, and megakaryocyte (GEMM).

Humanized Mice and Tissue Processing

NOD.Cg-Prkdc^{scid}Il2rg^{tm1Wjl}/Szj (NOD SCID gamma$^{-/-}$, NSG) mice were purchased from the Jackson Laboratory (Bar Harbor, ME) and bred in-house under approved protocols in pathogen-free housing conditions. Neonatal mice between 1 and 3 days post-birth received 150 cGy of radiation, followed 3–4 hr later by a single intrahepatic injection of 1 million CD34$^+$ cells resuspended in 30 μL of PBS containing 1% heparin (Abraxis BioScience, Los Angeles, CA). Blood samples were collected by retro-orbital puncture beginning at week 8 post-engraftment. Red blood cells were removed by incubation in BD FACS Lysing Solution (BD Biosciences, Franklin Lakes, NJ), which was then diluted in PBS prior to analysis by flow cytometry. At the end of the study, animals were sacrificed, and lymphoid tissues were harvested for analysis and dissociated using 70-μm filters.

HIV Challenge and Viremia Quantification

Between 19 and 23 weeks, mice with evidence of bNAb secretion in the peripheral blood and GFP mice as controls were challenged intraperitoneally with 1×10^5 IU of HIV-1 BaL (obtained through the NIH AIDS Reagent Program, Division of AIDS, NIAID, NIH, reference 510, from Dr. Suzanne Gartner, Dr. Mikulas Popovic, and Dr. Robert Gallo) that was previously propagated in PM1 cells (NIH ARP, reference 828) and titered using standard protocol for GHOST

X4/R5 cells (NIH ARP, reference 3942). Viral RNA was extracted from mouse serum or tissue culture supernatant using the QIAamp Viral RNA Mini Kit (QIAGEN, Hilden, Germany) as previously described.[26] In brief, viral RNA was then analyzed using the TaqMan RNA-to-Ct 1-Step Kit (Thermo Fisher) using primer and probes specific to the long terminal repeat (LTR) region (F, 5′-GCCTCAATAAAGCTTGCCTTGAG-3′; R, 5′-GGCGCCACTGCTAGAGATTTTC-3′; probe, FAM 5′-AAGTAGTGTGTGCCCGTCTGTTRTKTGACT-3′ TAMARA). Plates were analyzed on an ABI TaqMan 7500 real-time PCR system (Thermo Fisher).

Ethics Statement

All animal studies were carried out in compliance with approved protocols (1864) by the Institutional Animal Care and Use Committee (IACUC) at the Fred Hutchinson Cancer Research Center.

Flow Cytometry

Lentiviral transduction was assessed by flow cytometry quantification of GFP expression as soon as 1 day post-transduction. HSPCs were also stained with anti-human CD45 V450 (BD, clone HI30), CD34 Texas-Red (BD Biosciences, clone 563), CD133 PE (Miltenyi, clone AC133), CD90 PECy7 (BD Biosciences, clone 5E10), and CD45RA APC-Cy7 (BD Biosciences, clone 5H9). Stained cells were acquired on an LSRII (BD Biosciences). Blood and tissue samples were stained with appropriate antibodies for 15 min at room temperature and analyzed by flow cytometry for expression of mouse and human CD45 (BD Biosciences, clones 30-F11 and 2D1, respectively), CD3 (BD Biosciences, clone UCHT1), CD4 (BD Biosciences, clone RPA-T4), CD8 (BD Biosciences, clone SK1), CD14 (BD Biosciences, clone M5E2), and CD20 (BD Biosciences, clone 2H7). Stained cells were acquired on a FACS Canto II (BD Biosciences). Bone marrow was also stained with CD34-APC (clone 581). Data collection was performed on up to 20,000 cells in the viable cell population for blood and 100,000 cells for tissues. All data were analyzed using FlowJo software v10.1 (Tree Star).

Cell Sorting and RNA Extraction

Total RNA was extracted from unsorted or sorted white blood cells. In brief, peripheral blood was collected from humanized mice, red blood cells were lysed as described above, and white blood cells were stained with mouse CD45 (clone 30-F11), human CD45 (clone 2D1), human CD3 (clone UCHT1), human CD20 (clone 2H7), and human CD14 (clone M5E2) antibodies and sorted using a BD FACS Aria II cell sorter (BD Biosciences). RNA was immediately extracted from sorted cells using the Arcturus PicoPure RNA isolation kit (Thermo Fisher Scientific) in combination with the RNase-free DNase set (QIAGEN, Hilden, Germany) according to the manufacturer's instructions and stored at −80°C until further use. mRNA was reverse transcribed using the SuperScript III First-Strand Synthesis kit for RT-PCR (Thermo Fisher Scientific, Waltham, MA) and PCR amplified with the Platinum PCR SuperMix High Fidelity kit (Thermo Fisher Scientific, Waltham, MA) using the following primers: actin forward 5′-TCCTGTGGCATCGACGAAACT-3′ and reverse 5′-GAAGCATTTGCGGTGGACGAT-3′; PGT128 light chain variable region forward 5′-GCCCCCAAGCTCGTCATTTA-3′ and reverse 5′-AGTTGCCTACAAGTGAGCCG-3′; PGT128 heavy-chain variable region forward 5′- TTGGGAGTTTGTCCCATTGT-3′ and reverse 5′-GCCAATCCGTGTAGCGTAAA-3′; VRC01 light-chain variable region 5′-ACAGCCATCATCTCTTGTCGG-3′ and reverse 5′-TGAGATTGTAGTCTGGCCCC-3′; VRC01 heavy-chain variable region 5′-GTCGGGCTTCTGGATATGAA-3′ and reverse 5′-GCCGTGTCGTCTACTGTCAA-3′.

ELISA

Five micrograms of concanavalin A per well of a 96-well maxisorp plate (Thermo Fisher scientific, Waltham, MA) was incubated overnight at room temperature, followed by two washes with 0.05% PBS-Tween 20. The plates were then coated with 50 ng of HIV-1 BaL gp120 recombinant protein (NIH AIDS Reagent Program, Division of AIDS, NIAID, NIH) for 1 hr at room temperature, washed four times, then incubated in blocking buffer (5% milk-0.05% Tween 20 in PBS) for 1 hr at room temperature. Samples (cell-free supernatants or plasma) and standards were serially diluted in a U-bottom 96-well plate in blocking buffer, transferred to the maxisorp plate, incubated for 1 hr at room temperature and washed four times before the addition of anti-human peroxidase-conjugated rabbit anti-human immunoglobulin G (IgG) secondary antibody (Sigma-Aldrich A8792, 1:80,000 dilution) for 1 hr at room temperature. The plates were washed four times before addition of the 3,3',5,5' tetramethylbenzidine (TMB) solution (Sigma-Aldrich, St. Louis, MO) and incubated for 20 min at room temperature on an orbital shaker. The reaction was stopped by addition of 1 N H_2SO_4. The absorbance was read at 450 nm using a BioTek EL800 microplate absorbance reader (Biotek, Winooski, VT). Standard curves for antibody quantification were established using purified monoclonal antibodies (anti-HIV-1 gp120 monoclonal VRC01, from Dr. John Mascola, NIH AIDS Reagent Program, Division of AIDS, NIAID, NIH, and anti-HIV-1 gp120 monoclonal PGT128, from Dr. Denis Burton, IAVI consortium). GFP-only mice were used as negative controls to set the threshold for each experiment. Plasma samples were considered as positive if the absorbance was at least two-fold higher than the plasma from GFP-only mice.

Neutralization Assay

Cell-free supernatants were obtained by centrifugation of cell culture supernatants for 5 min at 1,000 × g. The collected supernatants were purified using ZebaSpin Desalting Columns (Thermo Fisher Scientific, Waltham, MA) followed by Melon gel IgG spin purification kit (Thermo Fisher Scientific, Waltham, MA). 2.5×10^4 TZM-bl cells were plated in a TC-treated flat-bottom 96-well plate and allowed to adhere for 6 hr. Reference antibodies (VRC01 from the NIH AIDS Reagent Program, Dr. John Mascola and PGT128 from the IAVI consortium, Dr. Denis Burton), or purified cell-free supernatants were serially diluted in TZM-bl cell culture media in a U-bottom 96-well plate. HIV-1 BaL (NIH ARP, reference 510, from Dr. Suzanne Gartner, Dr. Mikulas Popovic and Dr. Robert Gallo) that was previously propagated in PM1 cells (NIH ARP, reference 3038) and titered using standard protocol for GHOST X4/R5 cells (NIH ARP, reference

3942), was added to the serially diluted antibodies or mock supernatant to reach a final 0.2 MOI when added to the target TZM-bl cells. Virus and antibody dilutions were mixed and incubated for 1 hr at 37°C. Untreated and antibody-treated virus samples were then transferred onto the target TZM-bl cells and incubated overnight at 37°C. Media was changed 12 hr following infection. Forty-eight hours post-infection, the cells were lysed with 50 μL of cell culture lysis reagent from the luciferase assay system kit according to the manufacturer's instructions (Promega, Madison, WI), and luciferase activity was read using a Berthold microplate luminometer (Berthold, Oak Ridge, TN). Neutralization activity was calculated relative to the virus infectivity in the absence of antibodies, referenced as 100%.

Immunohistochemistry

Single-label immunohistochemical staining against GFP was utilized to confirm the presence of gene-modified cells in humanized mouse tissues. Formalin-fixed paraffin-embedded sections were deparaffinized in xylene and rehydrated through a graded ethanol series followed by deionized water. Sections were treated with 3% hydrogen peroxide for 15 min at room temperature to block endogenous peroxidase activity, and antigen retrieval was accomplished by boiling the sections in a commercial rice cooker (95°C–97°C) for 20 min in Tris-EDTA buffer (10 mM Tris base, 1mM EDTA solution, 0.05% Tween 20 [pH 9.0]). Tissue sections were blocked with a casein-based protein block for 20 min at room temperature (X0909; Dako, Carpinteria, CA) prior to immunostaining with rabbit anti-GFP primary antibody (A-11122; Invitrogen, Carlsbad, CA; 1:1,000) for 1 hr at room temperature in a humidified chamber. The primary antibody was diluted to an appropriate working concentration with a commercial antibody diluent (559148; Becton Dickinson, Franklin Lakes, NJ). Secondary antibody labeling was accomplished with a horse anti-rabbit IgG poly-horseradish peroxidase (HRP) (MP-7401; Vector Laboratories, Burlingame, CA), and antigen-antibody complexes were visualized with 3,3′ diaminobenzidine (DAB; 550880; Becton Dickinson, Franklin Lakes, NJ). Slides were counterstained with hematoxylin (S3302; Dako, Carpinteria, CA), dehydrated through a graded ethanol series followed by xylene, and mounted with permanent mounting media (SP15-100; Fisher Scientific, Hampton, NH). Sections were scanned with an Aperio ScanScope AT (Leica Biosystems, Wetzlar, Germany), and images were generated using HALO software (Indica Labs, Corrales, NM). Representative positive and negative control slides were processed in an identical manner, as well as with non-specific, isotype-matched rabbit antibody (08-6199; Invitrogen, Carlsbad, CA).

SUPPLEMENTAL INFORMATION

Supplemental Information includes eight figures and can be found with this article online at https://doi.org/10.1016/j.ymthe.2018.09.017.

AUTHOR CONTRIBUTIONS

H.-P.K. is the principal investigator of the study. H.-P.K. designed the experiments and coordinated the overall execution of the project. A.-S.K. conceived, designed, and coordinated the experiments. K.G.H. coordinated and helped in designing the *in vivo* experiments. C.W.P. provided feedback and critical input. A.-S.K., K.G.H., I.M.-B.A., C.I., and M.A.G. performed and analyzed experimental data. A.S.K. wrote the manuscript, which was critically reviewed by C.W.P., K.G.H, and H.-P.K.

CONFLICTS OF INTEREST

The authors have no conflicts of interest.

ACKNOWLEDGMENTS

We thank Helen Crawford for help preparing and formatting this manuscript. We also thank Jerry Chen, Sarah Weitz, Melissa Comstock, and Don Parrilla for assistance with performing mouse procedures and general colony maintenance, Megan Atkins for processing and isolation of apheresis $CD34^+$ cells, and Martin Wohlfahrt, Don Gisch, and Madison Norton for producing lentiviral vectors. This work was supported in part by grants from the NIH (R21 AI110154, U19 AI096111, U19 HL129902, UM1 AI126623, and R01 HL116217) and the Fred Hutch Core Center Grant (CCSG P30 CA015704). H.-P.K. is a Markey Molecular Medicine Investigator and received support as the inaugural recipient of the Jose Carreras/E. Donnall Thomas Endowed Chair for Cancer Research and the Fred Hutch Endowed Chair for Cell and Gene Therapy.

REFERENCES

1. Mouton, J.P., Cohen, K., and Maartens, G. (2016). Key toxicity issues with the WHO-recommended first-line antiretroviral therapy regimen. Expert Rev. Clin. Pharmacol. *9*, 1493–1503.

2. Shah, A., Gangwani, M.R., Chaudhari, N.S., Glazyrin, A., Bhat, H.K., and Kumar, A. (2016). Neurotoxicity in the Post-HAART Era: Caution for the Antiretroviral Therapeutics. Neurotox. Res. *30*, 677–697.

3. Ouyang, Y., Yin, Q., Li, W., Li, Z., Kong, D., Wu, Y., Hong, K., Xing, H., Shao, Y., Jiang, S., et al. (2017). Escape from humoral immunity is associated with treatment failure in HIV-1-infected patients receiving long-term antiretroviral therapy. Sci. Rep. *7*, 6222.

4. Bolton, D.L., Pegu, A., Wang, K., McGinnis, K., Nason, M., Foulds, K., Letukas, V., Schmidt, S.D., Chen, X., Todd, J.P., et al. (2015). Human Immunodeficiency Virus Type 1 Monoclonal Antibodies Suppress Acute Simian-Human Immunodeficiency Virus Viremia and Limit Seeding of Cell-Associated Viral Reservoirs. J. Virol. *90*, 1321–1332.

5. Horwitz, J.A., Halper-Stromberg, A., Mouquet, H., Gitlin, A.D., Tretiakova, A., Eisenreich, T.R., Malbec, M., Gravemann, S., Billerbeck, E., Dorner, M., et al. (2013). HIV-1 suppression and durable control by combining single broadly neutralizing antibodies and antiretroviral drugs in humanized mice. Proc. Natl. Acad. Sci. USA *110*, 16538–16543.

6. Chun, T.W., Murray, D., Justement, J.S., Blazkova, J., Hallahan, C.W., Fankuchen, O., Gittens, K., Benko, E., Kovacs, C., Moir, S., and Fauci, A.S. (2014). Broadly neutralizing antibodies suppress HIV in the persistent viral reservoir. Proc. Natl. Acad. Sci. USA *111*, 13151–13156.

7. Bruel, T., Guivel-Benhassine, F., Amraoui, S., Malbec, M., Richard, L., Bourdic, K., Donahue, D.A., Lorin, V., Casartelli, N., Noël, N., et al. (2016). Elimination of HIV-1-infected cells by broadly neutralizing antibodies. Nat. Commun. *7*, 10844.

8. Halper-Stromberg, A., Lu, C.L., Klein, F., Horwitz, J.A., Bournazos, S., Nogueira, L., Eisenreich, T.R., Liu, C., Gazumyan, A., Schaefer, U., et al. (2014). Broadly neutralizing antibodies and viral inducers decrease rebound from HIV-1 latent reservoirs in humanized mice. Cell *158*, 989–999.

9. Balazs, A.B., Ouyang, Y., Hong, C.M., Chen, J., Nguyen, S.M., Rao, D.S., An, D.S., and Baltimore, D. (2014). Vectored immunoprophylaxis protects humanized mice from mucosal HIV transmission. Nat. Med. *20*, 296–300.

10. Caskey, M., Klein, F., Lorenzi, J.C., Seaman, M.S., West, A.P., Jr., Buckley, N., Kremer, G., Nogueira, L., Braunschweig, M., Scheid, J.F., et al. (2015). Viraemia suppressed in HIV-1-infected humans by broadly neutralizing antibody 3BNC117. Nature *522*, 487–491.

11. Deruaz, M., Moldt, B., Le, K.M., Power, K.A., Vrbanac, V.D., Tanno, S., Ghebremichael, M.S., Allen, T.M., Tager, A.M., Burton, D.R., and Luster, A.D. (2016). Protection of humanized mice from repeated intravaginal HIV challenge by passive immunization: A model for studying the efficacy of neutralizing antibodies in vivo. J. Infect. Dis. *214*, 612–616.

12. Lu, C.L., Murakowski, D.K., Bournazos, S., Schoofs, T., Sarkar, D., Halper-Stromberg, A., Horwitz, J.A., Nogueira, L., Golijanin, J., Gazumyan, A., et al. (2016). Enhanced clearance of HIV-1-infected cells by broadly neutralizing antibodies against HIV-1 in vivo. Science *352*, 1001–1004.

13. Lynch, R.M., Boritz, E., Coates, E.E., DeZure, A., Madden, P., Costner, P., Enama, M.E., Plummer, S., Holman, L., Hendel, C.S., et al.; VRC 601 Study Team (2015). Virologic effects of broadly neutralizing antibody VRC01 administration during chronic HIV-1 infection. Sci. Transl. Med. *7*, 319ra206.

14. Saunders, K.O., Pegu, A., Georgiev, I.S., Zeng, M., Joyce, M.G., Yang, Z.Y., Ko, S.Y., Chen, X., Schmidt, S.D., Haase, A.T., et al. (2015). Sustained delivery of a broadly neutralizing antibody in nonhuman primates confers long-term protection against Simian/Human Immunodeficiency Virus infection. J. Virol. *89*, 5895–5903.

15. Schoofs, T., Klein, F., Braunschweig, M., Kreider, E.F., Feldmann, A., Nogueira, L., Oliveira, T., Lorenzi, J.C., Parrish, E.H., Learn, G.H., et al. (2016). HIV-1 therapy with monoclonal antibody 3BNC117 elicits host immune responses against HIV-1. Science *352*, 997–1001.

16. Caskey, M., Schoofs, T., Gruell, H., Settler, A., Karagounis, T., Kreider, E.F., Murrell, B., Pfeifer, N., Nogueira, L., Oliveira, T.Y., et al. (2017). Antibody 10-1074 suppresses viremia in HIV-1-infected individuals. Nat. Med. *23*, 185–191.

17. Bournazos, S., Klein, F., Pietzsch, J., Seaman, M.S., Nussenzweig, M.C., and Ravetch, J.V. (2014). Broadly neutralizing anti-HIV-1 antibodies require Fc effector functions for in vivo activity. Cell *158*, 1243–1253.

18. Nishimura, Y., Gautam, R., Chun, T.W., Sadjadpour, R., Foulds, K.E., Shingai, M., Klein, F., Gazumyan, A., Golijanin, J., Donaldson, M., et al. (2017). Early antibody therapy can induce long-lasting immunity to SHIV. Nature *543*, 559–563.

19. Ledgerwood, J.E., Coates, E.E., Yamshchikov, G., Saunders, J.G., Holman, L., Enama, M.E., DeZure, A., Lynch, R.M., Gordon, I., Plummer, S., et al.; VRC 602 Study Team (2015). Safety, pharmacokinetics and neutralization of the broadly neutralizing HIV-1 human monoclonal antibody VRC01 in healthy adults. Clin. Exp. Immunol. *182*, 289–301.

20. Gautam, R., Nishimura, Y., Pegu, A., Nason, M.C., Klein, F., Gazumyan, A., Golijanin, J., Buckler-White, A., Sadjadpour, R., Wang, K., et al. (2016). A single injection of anti-HIV-1 antibodies protects against repeated SHIV challenges. Nature *533*, 105–109.

21. Rudicell, R.S., Kwon, Y.D., Ko, S.Y., Pegu, A., Louder, M.K., Georgiev, I.S., Wu, X., Zhu, J., Boyington, J.C., Chen, X., et al.; NISC Comparative Sequencing Program (2014). Enhanced potency of a broadly neutralizing HIV-1 antibody in vitro improves protection against lentiviral infection in vivo. J. Virol. *88*, 12669–12682.

22. Mayer, K.H., Seaton, K.E., Huang, Y., Grunenberg, N., Isaacs, A., Allen, M., Ledgerwood, J.E., Frank, I., Sobieszczyk, M.E., Baden, L.R., et al.; HVTN 104 Protocol Team; and the NIAID HIV Vaccine Trials Network (2017). Safety, pharmacokinetics, and immunological activities of multiple intravenous or subcutaneous doses of an anti-HIV monoclonal antibody, VRC01, administered to HIV-uninfected adults: Results of a phase 1 randomized trial. PLoS Med. *14*, e1002435.

23. Sessa, M., Lorioli, L., Fumagalli, F., Acquati, S., Redaelli, D., Baldoli, C., Canale, S., Lopez, I.D., Morena, F., Calabria, A., et al. (2016). Lentiviral haemopoietic stem-cell gene therapy in early-onset metachromatic leukodystrophy: an ad-hoc analysis of a non-randomised, open-label, phase 1/2 trial. Lancet *388*, 476–487.

24. Joseph, A., Zheng, J.H., Chen, K., Dutta, M., Chen, C., Stiegler, G., Kunert, R., Follenzi, A., and Goldstein, H. (2010). Inhibition of in vivo HIV infection in humanized mice by gene therapy of human hematopoietic stem cells with a lentiviral vector encoding a broadly neutralizing anti-HIV antibody. J. Virol. *84*, 6645–6653.

25. Radtke, S., Adair, J.E., Giese, M.A., Chan, Y.Y., Norgaard, Z.K., Enstrom, M., Haworth, K.G., Schefter, L.E., and Kiem, H.P. (2017). A distinct hematopoietic stem cell population for rapid multilineage engraftment in nonhuman primates. Sci. Transl. Med. *9*, eaan1145.

26. Haworth, K.G., Ironside, C., Norgaard, Z.K., Obenza, W.M., Adair, J.E., and Kiem, H.P. (2017). In vivo murine-matured human CD3+ cells as a preclinical model for T cell-based immunotherapies. Mol. Ther. Methods Clin. Dev. *6*, 17–30.

27. Matzner, U., Hartmann, D., Lüllmann-Rauch, R., Coenen, R., Rothert, F., Månsson, J.E., Fredman, P., D'Hooge, R., De Deyn, P.P., and Gieselmann, V. (2002). Bone marrow stem cell-based gene transfer in a mouse model for metachromatic leukodystrophy: effects on visceral and nervous system disease manifestations. Gene Ther. *9*, 53–63.

28. Sergijenko, A., Langford-Smith, A., Liao, A.Y., Pickford, C.E., McDermott, J., Nowinski, G., Langford-Smith, K.J., Merry, C.L., Jones, S.A., Wraith, J.E., et al. (2013). Myeloid/Microglial driven autologous hematopoietic stem cell gene therapy corrects a neuronopathic lysosomal disease. Mol. Ther. *21*, 1938–1949.

29. Biffi, A., Capotondo, A., Fasano, S., del Carro, U., Marchesini, S., Azuma, H., Malaguti, M.C., Amadio, S., Brambilla, R., Grompe, M., et al. (2006). Gene therapy of metachromatic leukodystrophy reverses neurological damage and deficits in mice. J. Clin. Invest. *116*, 3070–3082.

30. Gardner, M.R., Kattenhorn, L.M., Kondur, H.R., von Schaewen, M., Dorfman, T., Chiang, J.J., Haworth, K.G., Decker, J.M., Alpert, M.D., Bailey, C.C., et al. (2015). AAV-expressed eCD4-Ig provides durable protection from multiple SHIV challenges. Nature *519*, 87–91.

31. Moldt, B., Rakasz, E.G., Schultz, N., Chan-Hui, P.Y., Swiderek, K., Weisgrau, K.L., Piaskowski, S.M., Bergman, Z., Watkins, D.I., Poignard, P., and Burton, D.R. (2012). Highly potent HIV-specific antibody neutralization in vitro translates into effective protection against mucosal SHIV challenge in vivo. Proc. Natl. Acad. Sci. USA *109*, 18921–18925.

32. Bar, K.J., Sneller, M.C., Harrison, L.J., Justement, J.S., Overton, E.T., Petrone, M.E., Salantes, D.B., Seamon, C.A., Scheinfeld, B., Kwan, R.W., et al. (2016). Effect of HIV Antibody VRC01 on Viral Rebound after Treatment Interruption. N. Engl. J. Med. *375*, 2037–2050.

33. Sullivan, N., Sun, Y., Binley, J., Lee, J., Barbas, C.F., 3rd, Parren, P.W., Burton, D.R., and Sodroski, J. (1998). Determinants of human immunodeficiency virus type 1 envelope glycoprotein activation by soluble CD4 and monoclonal antibodies. J. Virol. *72*, 6332–6338.

34. Walker, L.M., Huber, M., Doores, K.J., Falkowska, E., Pejchal, R., Julien, J.P., Wang, S.K., Ramos, A., Chan-Hui, P.Y., Moyle, M., et al.; Protocol G Principal Investigators (2011). Broad neutralization coverage of HIV by multiple highly potent antibodies. Nature *477*, 466–470.

35. Klein, F., Halper-Stromberg, A., Horwitz, J.A., Gruell, H., Scheid, J.F., Bournazos, S., Mouquet, H., Spatz, L.A., Diskin, R., Abadir, A., et al. (2012). HIV therapy by a combination of broadly neutralizing antibodies in humanized mice. Nature *492*, 118–122.

36. Kong, R., Louder, M.K., Wagh, K., Bailer, R.T., deCamp, A., Greene, K., Gao, H., Taft, J.D., Gazumyan, A., Liu, C., et al. (2015). Improving neutralization potency and breadth by combining broadly reactive HIV-1 antibodies targeting major neutralization epitopes. J. Virol. *89*, 2659–2671.

37. Bournazos, S., Gazumyan, A., Seaman, M.S., Nussenzweig, M.C., and Ravetch, J.V. (2016). Bispecific Anti-HIV-1 Antibodies with Enhanced Breadth and Potency. Cell *165*, 1609–1620.

38. Xu, L., Pegu, A., Rao, E., Doria-Rose, N., Beninga, J., McKee, K., Lord, D.M., Wei, R.R., Deng, G., Louder, M., et al. (2017). Trispecific broadly neutralizing HIV antibodies mediate potent SHIV protection in macaques. Science *358*, 85–90.

39. Sanhadji, K., Grave, L., Touraine, J.L., Leissner, P., Rouzioux, C., Firouzi, R., Kehrli, L., Tardy, J.C., and Mehtali, M. (2000). Gene transfer of anti-gp41 antibody and CD4 immunoadhesin strongly reduces the HIV-1 load in humanized severe combined immunodeficient mice. AIDS *14*, 2813–2822.

40. Hur, E.M., Patel, S.N., Shimizu, S., Rao, D.S., Gnanapragasam, P.N., An, D.S., Yang, L., and Baltimore, D. (2012). Inhibitory effect of HIV-specific neutralizing IgA on mucosal transmission of HIV in humanized mice. Blood *120*, 4571–4582.

41. Yu, K.K., Aguilar, K., Tsai, J., Galimidi, R., Gnanapragasam, P., Yang, L., and Baltimore, D. (2012). Use of mutated self-cleaving 2A peptides as a molecular rheostat to direct simultaneous formation of membrane and secreted anti-HIV immunoglobulins. PLoS ONE *7*, e50438.

42. Fusil, F., Calattini, S., Amirache, F., Mancip, J., Costa, C., Robbins, J.B., Douam, F., Lavillette, D., Law, M., Defrance, T., et al. (2015). A lentiviral vector allowing physiologically regulated membrane-anchored and secreted antibody expression depending on B-cell maturation status. Mol. Ther. *23*, 1734–1747.

43. Chang, A.H., Stephan, M.T., Lisowski, L., and Sadelain, M. (2008). Erythroid-specific human factor IX delivery from in vivo selected hematopoietic stem cells following nonmyeloablative conditioning in hemophilia B mice. Mol. Ther. *16*, 1745–1752.

44. Roybal, K.T., Williams, J.Z., Morsut, L., Rupp, L.J., Kolinko, I., Choe, J.H., Walker, W.J., McNally, K.A., and Lim, W.A. (2016). Engineering T cells with customized therapeutic response programs using synthetic notch receptors. Cell *167*, 419–432.e16.

45. Peterson, C.W., Benne, C., Polacino, P., Kaur, J., McAllister, C.E., Filali-Mouhim, A., Obenza, W., Pecor, T.A., Huang, M.L., Baldessari, A., et al. (2017). Loss of immune homeostasis dictates SHIV rebound after stem-cell transplantation. JCI Insight *2*, e91230.

46. Murooka, T.T., Deruaz, M., Marangoni, F., Vrbanac, V.D., Seung, E., von Andrian, U.H., Tager, A.M., Luster, A.D., and Mempel, T.R. (2012). HIV-infected T cells are migratory vehicles for viral dissemination. Nature *490*, 283–287.

47. Petrovas, C., Ferrando-Martinez, S., Gerner, M.Y., Casazza, J.P., Pegu, A., Deleage, C., Cooper, A., Hataye, J., Andrews, S., Ambrozak, D., et al. (2017). Follicular CD8 T cells accumulate in HIV infection and can kill infected cells in vitro via bispecific antibodies. Sci. Transl. Med. *9*, eaag2285.

48. Brodie, S.J., Lewinsohn, D.A., Patterson, B.K., Jiyamapa, D., Krieger, J., Corey, L., Greenberg, P.D., and Riddell, S.R. (1999). In vivo migration and function of transferred HIV-1-specific cytotoxic T cells. Nat. Med. *5*, 34–41.

49. Kiniry, B.E., Li, S., Ganesh, A., Hunt, P.W., Somsouk, M., Skinner, P.J., Deeks, S.G., and Shacklett, B.L. (2017). Detection of HIV-1-specific gastrointestinal tissue resident CD8(+) T-cells in chronic infection. Mucosal Immunol. *11*, 909–920.

50. Kuhlmann, A.S., Peterson, C.W., and Kiem, H.P. (2018). Chimeric antigen receptor T-cell approaches to HIV cure. Curr. Opin. HIV AIDS *13*, 446–453.

51. Ananworanich, J., McSteen, B., and Robb, M.L. (2015). Broadly neutralizing antibody and the HIV reservoir in acute HIV infection: a strategy toward HIV remission? Curr. Opin. HIV AIDS *10*, 198–206.

52. Adair, J.E., Waters, T., Haworth, K.G., Kubek, S.P., Trobridge, G.D., Hocum, J.D., Heimfeld, S., and Kiem, H.P. (2016). Semi-automated closed system manufacturing of lentivirus gene-modified haematopoietic stem cells for gene therapy. Nat. Commun. *7*, 13173.